Quantitative interpretation using facies-based seismic inversion

Ehsan Zabihi Naeini[1] and Russell Exley[2]

Abstract

Quantitative interpretation (QI) is an important part of successful exploration, appraisal, and development activities. Seismic amplitude variation with offset (AVO) provides the primary signal for the vast majority of QI studies allowing the determination of elastic properties from which facies can be determined. Unfortunately, many established AVO-based seismic inversion algorithms are hindered by not fully accounting for inherent subsurface facies variations and also by requiring the addition of a preconceived low-frequency model to supplement the limited bandwidth of the input seismic. We apply a novel joint impedance and facies inversion applied to a North Sea prospect using broadband seismic data. The focus was to demonstrate the significant advantages of inverting for each facies individually and iteratively determine an optimized low-frequency model from facies-derived depth trends. The results generated several scenarios for potential facies distributions thereby providing guidance to future appraisal and development decisions.

Introduction

Derisking via quantitative interpretation (QI) is an essential part of successful hydrocarbon exploration and appraisal. In ideal circumstances, QI using amplitude variation with offset (AVO) inversion can be used to identify lithologies, indicate pore fluid fill, and determine net rock volume. However, the detail that can be extracted from a conventional AVO inversion workflow is limited by the averaging effects of not taking into account facies variations and adopting a simplified and rigid low-frequency model. To overcome this, Kemper and Gunning (2014) introduced an inversion algorithm that iteratively updates the low-frequency model input and in doing so ultimately outputs an optimized facies model and the associated elastic properties. The detail provided by the described joint impedance and facies-based inversion allows operators to pursue reservoir targets with increased confidence by quantifying facies distributions, reservoir geometries, and volumetrics. An example is shown here using a broadband long-offset seismic data set, broadband well tie, and wavelet estimation, followed by the newly developed facies-based seismic inversion.

The case study in this paper centers on a Paleocene discovery, known as Avalon, in block 21/6b of the UK Central North Sea located at the northwestern edge of the Central Graben just south of the Buchan Field. The discovery consisted of an 85 ft column of oil in good-quality sands and was initially defined using conventional simultaneous prestack inversion. The reservoir sands lie within the proximal part of the prolific northwest to southeast late Paleocene Forties and Cromarty depositional trend. This fairway includes the giant Forties Field. In general, Cromarty and Forties members have high porosities, high net-to-gross and, as a result of these rock properties, the reservoirs provide an ideal natural laboratory for applying AVO-based inversion techniques.

Method

Typical QI workflows consist of rock-physics analyses, fluid substitution, and seismic forward modeling, followed by the essential steps of seismic data conditioning, well tying, and subsequent inversion to elastic properties, with the eventual derivation of the facies. The example in this paper introduces two technologies that have been combined as part of a new QI workflow. The first was using a broadband, constant-phase well tie technique to estimate wavelets, and the second was inverting the seismic using a novel facies-based Bayesian inversion technique designed to analyze the distribution of reservoir bodies.

Input seismic data and bandwidth considerations

Broadband seismic data, in which the influence of the ghost reflections has been removed to avoid “notching” of the frequency spectrum, provides significant benefits compared with conventional band-limited data. However, reflectivity sections with an abundance of low-frequency signal will visually mask higher frequency signal,

[1]Ikon Science, London, UK. E-mail: enaeini@ikonscience.com.
[2]Summit Exploration & Production Ltd., London, UK. E-mail: rexley@summiteandp.com.
Manuscript received by the Editor 4 October 2016; revised manuscript received 13 December 2016; published online 09 March 2017. This paper appears in *Interpretation*, Vol. 5, No. 3 (August 2017); p. SL1–SL8, 8 FIGS.
http://dx.doi.org/10.1190/INT-2016-0178.1.

which is often the key to interpretation, providing an image that visually appears to be degraded in resolution and amplitude variations. Figure 1 shows a full stack section from a conventional processing flow and the equivalent section from a broadband processing flow. The application of a simple whitening operator to balance the frequency content of the broadband data demonstrates that the higher frequency signal is masked, but it is not removed, by the dominance of the low-frequency signal. This observation of high-frequency masking could be misleading when interpreting using only reflectivity seismic sections. However, this undesirable effect is automatically removed (deconvolved) by the inversion process provided suitable broadband wavelets are used for well ties.

Broadband well tie and wavelet estimation

Determining accurate and reliable well ties with broadband seismic is a problematic but essential initial step in the QI inversion workflow. Zabihi Naeini et al. (2016a) demonstrate an example of the importance of an accurate well tie (and therefore accurate wavelet estimation) for inversion specifically when using broadband seismic data. The problem of wavelet estimation for well ties to broadband seismic data arises because the length (in time) of the well logs is often inadequate to provide sufficient constraints on the low-frequency content of the resulting wavelet. Zabihi Naeini et al. (2016b) discuss this problem in detail and propose three different solutions. This study used one of their proposed wavelet estimation techniques — the parametric constant-phase method — to tie the prestack seismic to the well and subsequently use the wavelets for inversion. This approach uses a constant-phase approximation over the entire seismic bandwidth and therefore limits the degrees of freedom. Constant phase has some empirical basis because postprocessing the phase of the seismic wavelet should be approximately constant across the seismic bandwidth. This method is especially suitable when only a short log length is available because allowing the phase to vary with frequency could be unreliable. The constant phase is estimated us-

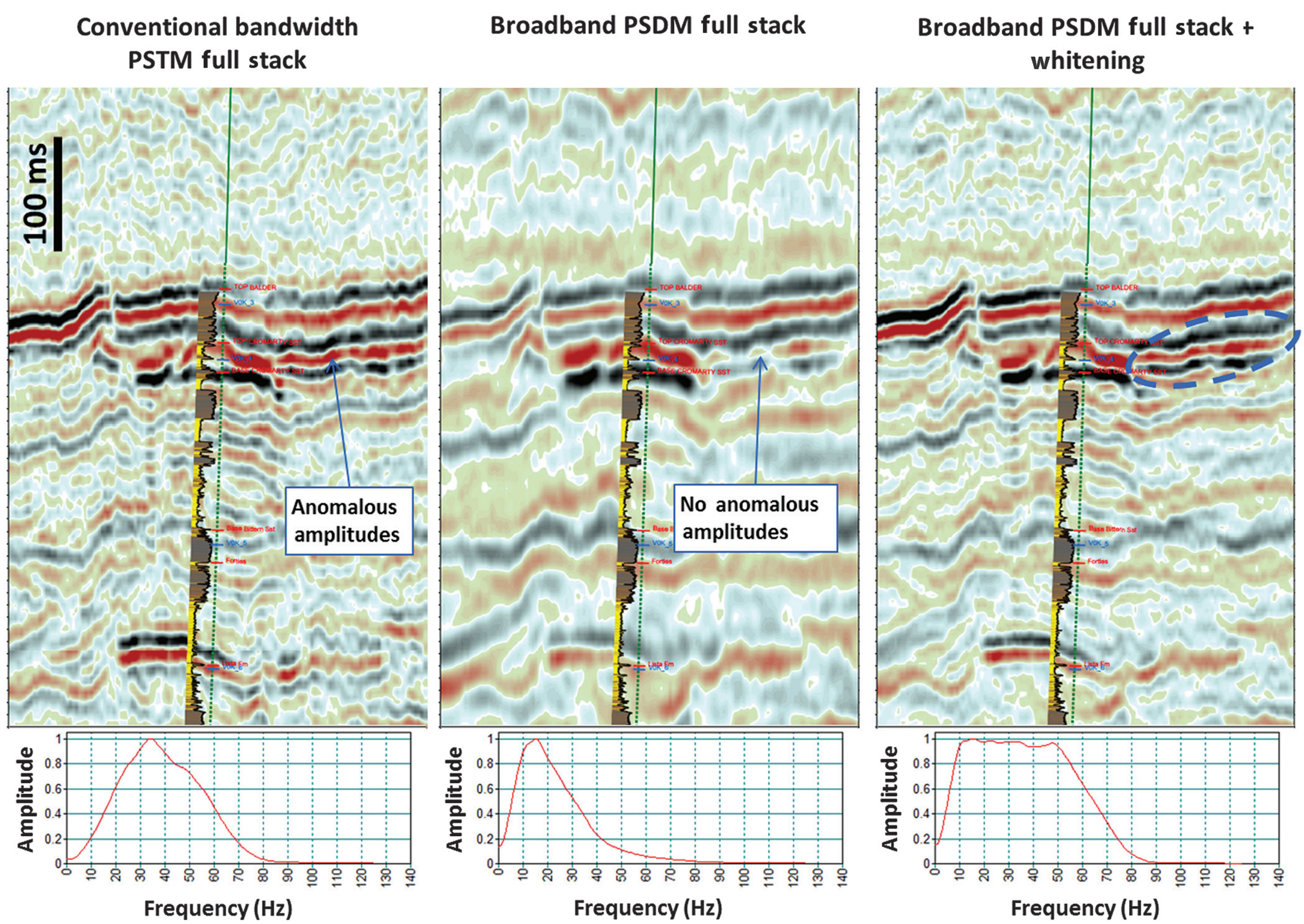

Figure 1. Full-stack sections from a transect across Avalon's reflectivity anomaly and the corresponding amplitude spectra for band-limited, broadband, and whitened broadband data are shown. The Vshale log for "well 2" is also shown. By applying a whitening operator to the broadband data, the imbalance between the low and high frequencies is reduced thus visually recovering some of the higher frequency features and amplitude variations (circled), which had been masked by the dominant low-frequency signal. The inversion process effectively also recovers the masked high-frequency signal through deconvolution without the need for whitening. Display in "SEG Normal" polarity (trough/red equals decreased impedance). Seismic data are courtesy of CGG.

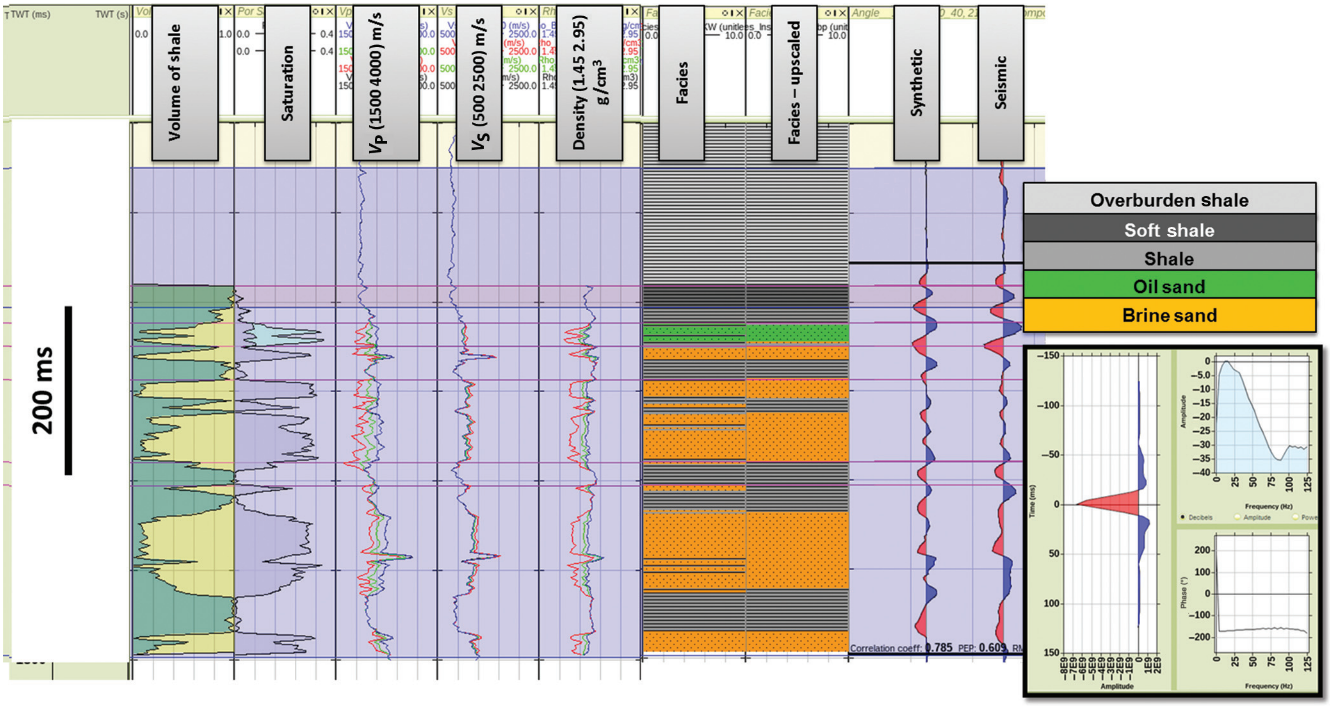

Figure 2. Panels of petrophysical and elastic properties including the brine (blue), oil (green), and gas (red)-saturated cases from the discovery well (well 2). Petrophysically derived facies before and after up-scaling are also shown in sixth and seventh panel, which were used to QC the inverted facies. The well tie panel is the last panel along with the estimated wavelet for the mid-angle stack. The polarity of the wavelet is "SEG Reverse" polarity (peak/blue equals decreased impedance).

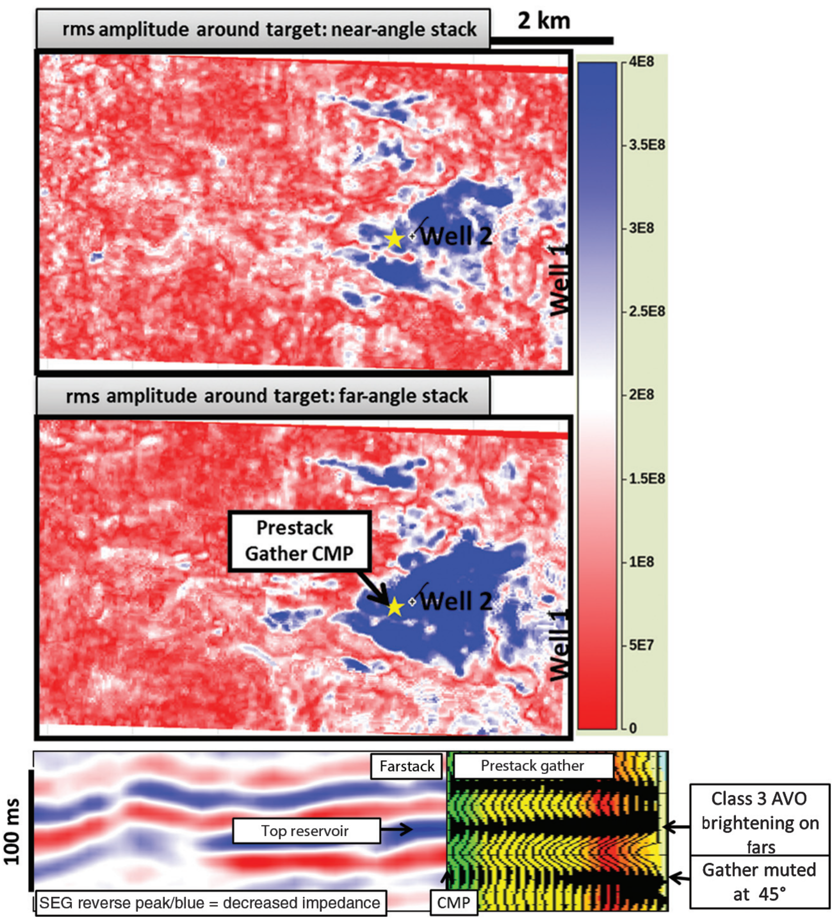

Figure 3. Reservoir rms amplitude maps from near- and far-angle stacks through the main reservoir interval. The Avalon anomaly is clearly bright on the near and even more so on the far offsets producing a characteristic class 3 AVO response. A typical prestack gather response (below) also indicates increased brightening on the far-offsets again consistent with a class 3 AVO response. Seismic data are courtesy of CGG.

ing a least-squares-based method over a long but tapered interval of seismic data to derive a stable amplitude spectrum using multiple traces around available wells.

Facies-based seismic inversion

Facies-based seismic inversion, in which the low-frequency model is a product of the inversion process itself, is first introduced by Kemper and Gunning (2014). The low-frequency model is constrained by per-facies depth-trended rock-physics models (RPMs; describing the depth-dependent Vp, Vs, and rho for each facies), the resultant facies distribution, and the match to the seismic.

In practice, seismic forward modeling and seismic inversion, both of which are part of a QI workflow and mathematically are reverse operations, have the same purpose: to understand the seismic signal and to predict subsurface facies and properties. In seismic forward modeling, understanding the facies distribution is crucial, because per-facies RPMs can be used to transform rock properties (e.g., porosity, volume of shale, hydrocarbon saturation) to elastic quantities (impedances), from which seismic can be synthesized using a variety of techniques and iteratively compared with recorded seismic data. Seismic inversion does just the opposite: An operator converts the seismic to impedances and/or rock properties as part of an optimization loop by repeatedly updating the model and forward modeling until it adequately fits the seismic data (this is model-based seismic inversion). However, there is often a disconnect between seismic forward modeling and seismic inversion in that a typical forward model takes facies into account, whereas facies are not incorporated in the forward modeling as part of conventional model-based seismic inversion. How can facies be a key quantity of forward modeling yet be ignored in forward modeling as part of seismic inversion? This conundrum provided the motivation to incorporate facies within the seismic inversion process. In what follows we briefly explain the standard model-based seismic inversion process and then the new facies-aware approach.

Standard model-based simultaneous inversion

In model-based inversion, we start with what is commonly called the "low-frequency model" (LFM) of impedances (e.g., compressional velocity Vp, shear velocity Vs, and density ρ), to account for the fact that band limited and, to a lesser extent, broadband seismic lack a low-frequency signal. It is worth noting that the quality of this LFM is often much more important than the actual inversion algorithm used. There are many such algorithms available, but in essence the seismic response is synthesized from the LFM and compared with the actual seismic. To reduce the misfit, the LFM is repeatedly

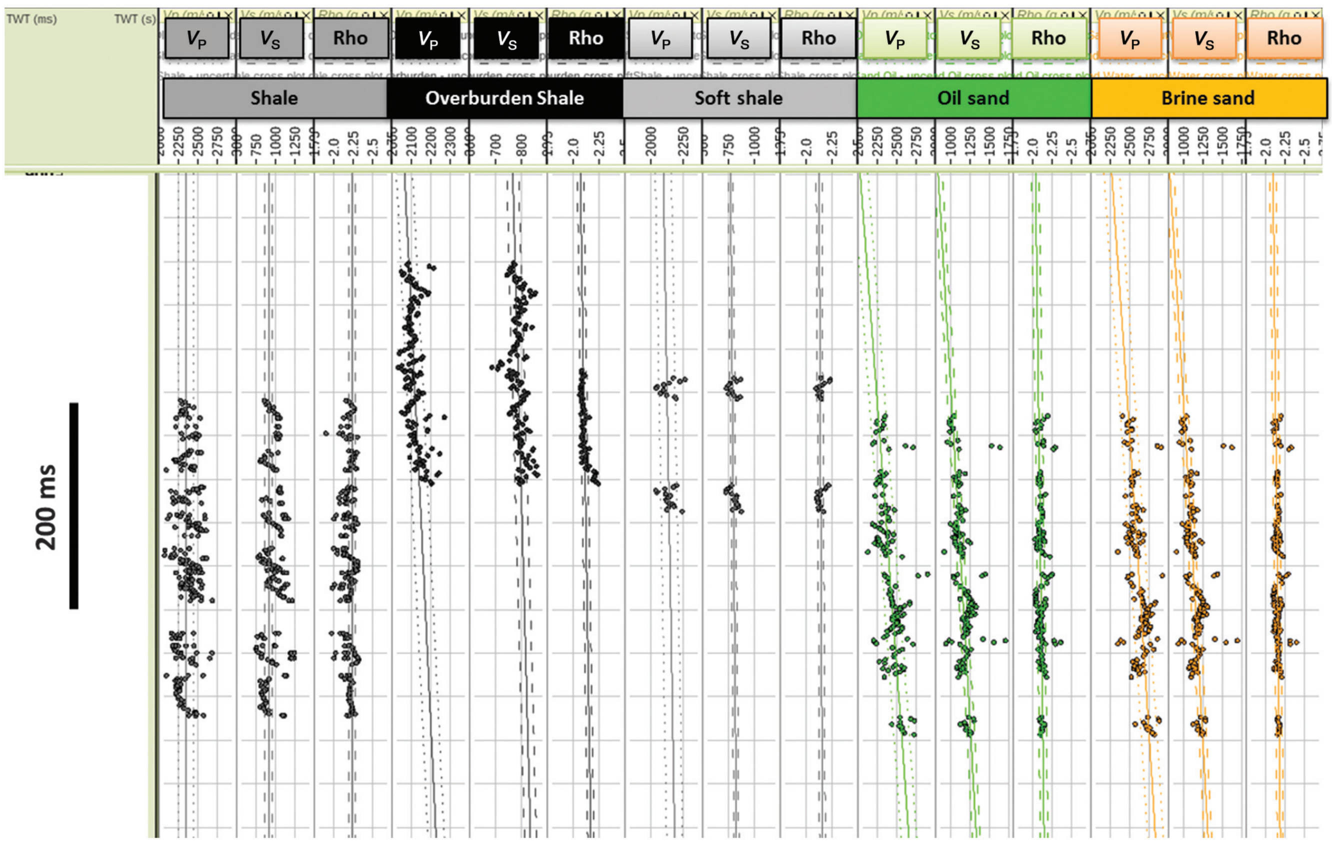

Figure 4. Depth-trended RPMs for each facies displayed in the depth domain (as opposed to the crossplot domain; see Figure 7). The dashed lines show the error bounds for each of the depth trends and also represent the constraints for which any given facies may be inverted to. Correlations between Vp and Vs and between Vp and rho were derived also as part of the RPMs (not shown).

updated, seismic resynthesized (using forward modeling), and recompared. Once the misfit is minimized, the process stops and the last model of impedances is the inversion result. Facies are not considered at any point in this process.

The problem with the above process is in the construction of the initial LFM, the most important input to this process. The starting model should have a gently varying vertical profile of sand impedance values in which sand is present (typically hardening because of compaction), and the same for other facies. But prior to the inversion, the location of the various facies is of course unknown; hence, it is not possible to assign the correct initial impedance value to the LFM at any given point. In practice, we end up with a compromise of impedance values (e.g., average impedance of different facies) unrepresentative of any particular facies, which degrades the inversion result.

The problem of facies variations is particularly evident when building the LFM by interpolation of well impedance profiles along interpreted seismic horizons (the typical form of LFM construction). At one well, we may have sand of a particular seismo-stratigraphic age, and in another well, we may have shale of the same age. Interpolation between these two wells produces compromised, neither-sand-nor-shale impedance values in the LFM and the subsequent seismic inversion cannot correct this error of low-frequency input bias as the seismic lacks low-frequency signal.

A new approach: Facies-aware model-based inversion

To improve the construction of the LFM, we input multiple, simple LFMs, one for each expected facies (i.e., we overspecify the low-frequency information). In its simplest form, we plot impedance log data as a function of depth below an appropriate datum restricted to a particular facies, and then we fit a compaction curve to that data, complete with an assessment of uncertainty. In three dimensions, we can take the horizon representing the datum, and "hang" the compaction curve off that horizon at all trace locations.

In this new approach, the inversion derives models of initial impedances (from the seismic) and then determines the facies during each iteration of the optimization loop. The facies result depends on the last set of impedance results, but here we focus on how the impedance results (inverted from the seismic data) depend on the last facies result (of the previous iteration). For this step, an LFM of impedances is required; this is reconstructed at each iteration from the various per-facies LFMs as follows:

1) Start with an empty LFM.
2) Where the last, most up-to-date facies model indicates there is sand, copy the sand into the LFM, partially populating the LFM.
3) Repeat for the other facies until the LFM is entirely populated.

The final LFM is therefore not a static input as in standard model-based simultaneous inversion, but it is the seismically driven output of the new inversion system, which incorporates known facies. Therefore, the main outputs of the inversion are the elastic properties and facies. Kemper and Gunning (2014) describe the mechanics of this new algorithm more fully.

North Sea case study

In this study, the input seismic was conventionally acquired but broadband processed, which consisted of two important processing steps. First, a preimaging 3D source- and receiver-side deghosting technique (Wang et al., 2013), for broadening the bandwidth of the conventionally acquired towed streamer data, was used to remove the frequency notches caused by ghost

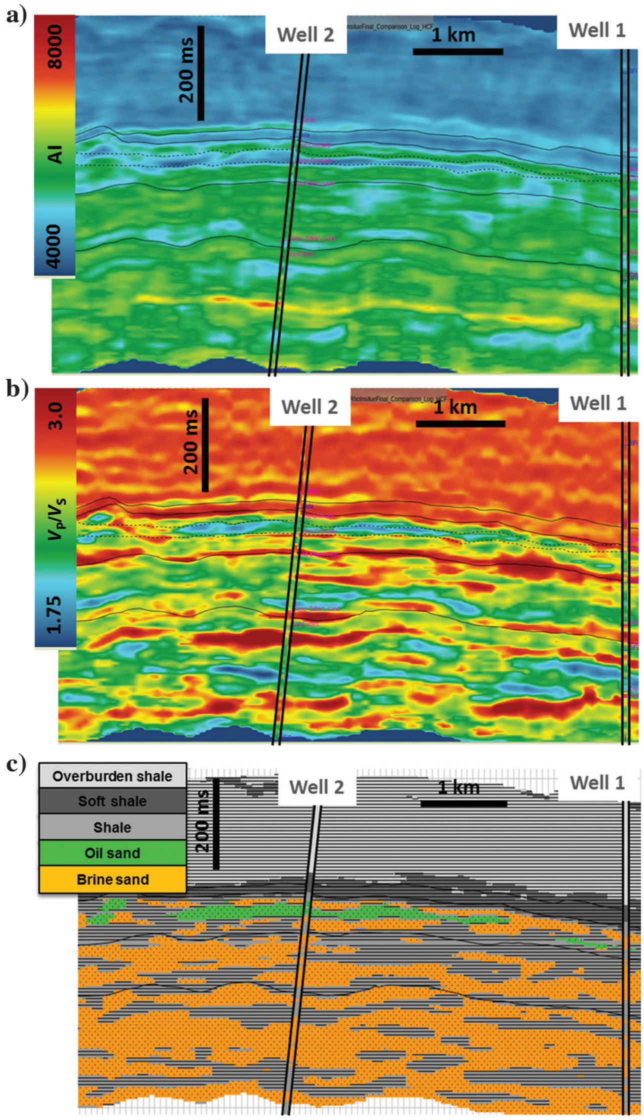

Figure 5. (a) Inverted AI (in g m/cm^3 s), (b) inverted Vp/Vs, and (c) inverted facies sections for an arbitrary line through the two calibration wells. The inversion was tested using similar 2D sections before application to the larger 3D data set in which a good match with the well logs can also be observed. The optimized match with the well logs was achieved by adjusting the prior depth trends and facies proportions, which are the inputs to the inversion optimization loop.

wavelet interference. Second, the processing workflow included a multilayer, nonlinear, slope tomography (Guillaume et al., 2013) to derive the velocity model for imaging and Kirchhoff prestack depth migration (PSDM) before stretching the data back to the time domain. Using such broadband seismic data increases the low- and high-frequency signal, thereby enhancing the resolution (Zabihi Naeini et al., 2015). Improved low frequencies within the seismic are especially important for seismic inversion because they reduce the dependency on the initial low-frequency information.

Figure 2 shows the well tie panel and the estimated wavelet, using the aforementioned constant-phase method, for the mid-angle stack. One can observe reasonable low-frequency decay on the amplitude spectrum obtained as part of the broadband wavelet estimation technique by using multitaper spectral smoothing and averaging over many traces around the well. The well tie workflow included a blind QC in which the wavelet was estimated at one well and used to tie the second well. After completing this process, a good-quality well tie can be observed with a crosscorrelation coefficient of 0.78 and a phase error of approximately 10°. Similar quality well ties were also achieved for the other angle stacks and at the other well in this study.

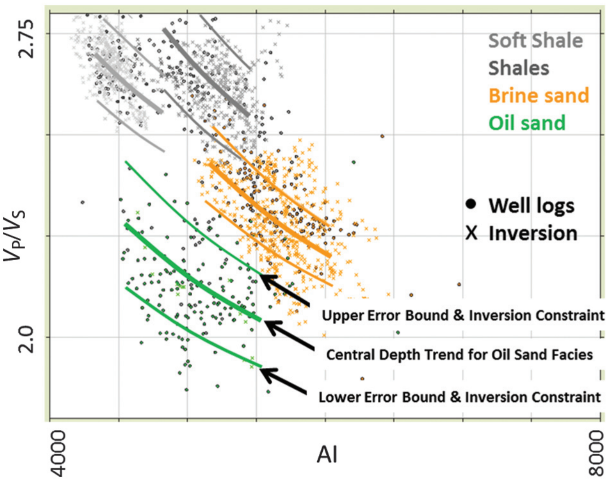

Figure 7. Depth-trended RPMs for each facies can be difficult to QC solely in the depth domain (Figure 4) and so can instead also be displayed on elastic crossplots as shown here. The depth-trended RPMs closely mimic typical compaction/porosity trends and also provide an indicative guide to the probability that each facies will be correctly identified. In this example, each of the facies are separated due to the high-porosity nature of the reservoir sands and distinct elastic properties of sands and shales. Also displayed are the error bounds for each depth-trended RPM that help constraining the inversion result.

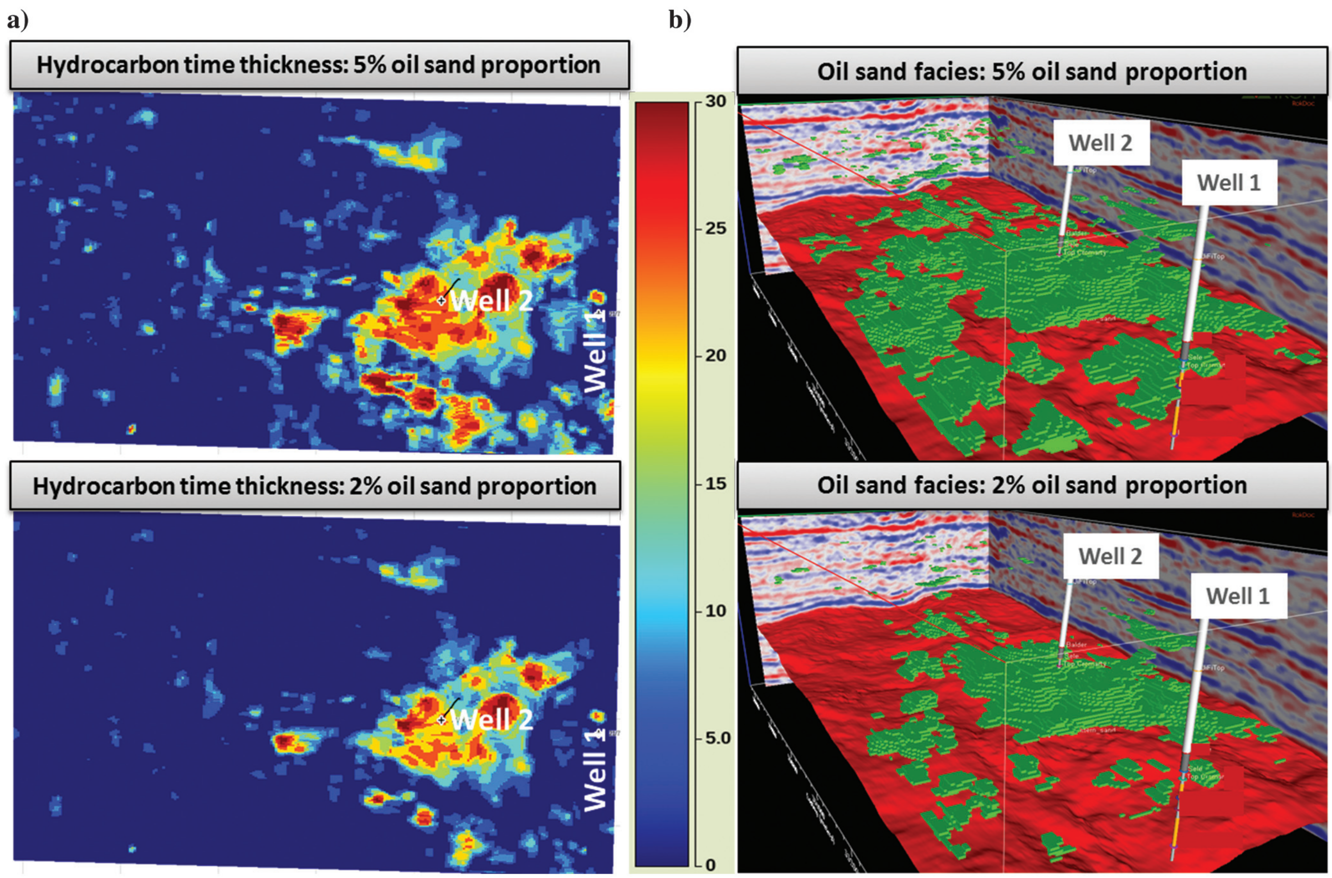

Figure 6. Facies probability proportions are prior inputs to the inversion and their sensitivity must be considered. This example shows two end-member scenarios used to explore a maximum (5%) and minimum (2%) oil-sand facies probability proportion. Panel (a) shows the hydrocarbon time thickness maps (in ms) and (b) shows the equivalent oil-sand facies distributions in three dimensions.

Initial rock-physics and forward-modeling studies revealed that the Avalon discovery exhibited a "textbook" class 3 AVO (Rutherford and Williams, 1989) anomaly from the top reservoir reflector. Figure 3 shows a typical prestack gather and resulting poststack rms amplitude maps from around the Avalon discovery for the near and far partial angle stacks. The main reservoir anomaly is evident around well 2.

The first and most critical step for the joint impedance and facies inversion was to derive impedance depth-trended RPMs for each facies. Three-dimensional low-frequency models were generated from these RPMs as explained earlier. Figure 4 shows RPMs for five facies: overburden hard shale, overburden soft shale, intrareservoir shale, oil sand, and brine sand. The overburden soft shale can also be observed in Figure 2 just above the reservoir. Separating the various shales into different facies types proved a critical factor to improve the inversion accuracy and distinguish soft shale from oil sands in particular.

Prior to running the inversion to derive facies and elastic properties in three dimensions, QC was performed in two dimensions. Figure 5 shows the resulting impedance (AI and Vp/Vs) and facies sections from an arbitrary line crossing both wells in this study, showing an optimized match at both wells. Post QC (Figure 6), we show two output scenarios, after running the inversion in three dimensions, for oil sand time thickness maps (constructed by summing the oil sand facies samples over the inversion window) for two end-member scenarios thereby investigating the sensitivity of prior facies probability proportions on hydrocarbon volume and distribution.

The final optimized inversion result (oil sand facies proportion 3%) provided an accurate correlation between measured (in the wells) and modeled (from the seismic inversion) acoustic and elastic impedances and the resulting facies. The inversion-derived facies output matched not only the oil column thickness but also the more difficult to differentiate brine-filled sands and shales encountered in the calibration wells. The inversion also successfully delineated a thin shale layer (observed in well 2) below the oil column that had a significant impact on the understanding of potential water drive during production. In addition, the connectivity of the oil sand facies and therefore the connectivity of potential satellite anomalies in three dimensions (Figure 6b) could be investigated across different inversion runs. The facies-specific output of this inversion technique also provided an ideal framework to quickly and efficiently generate static geocellular and dynamic reservoir models.

Inversion sensitivity

To further analyze the inversion sensitivity, the main parameters required to optimize this facies-aware inversion should be adjusted across several inversion runs to

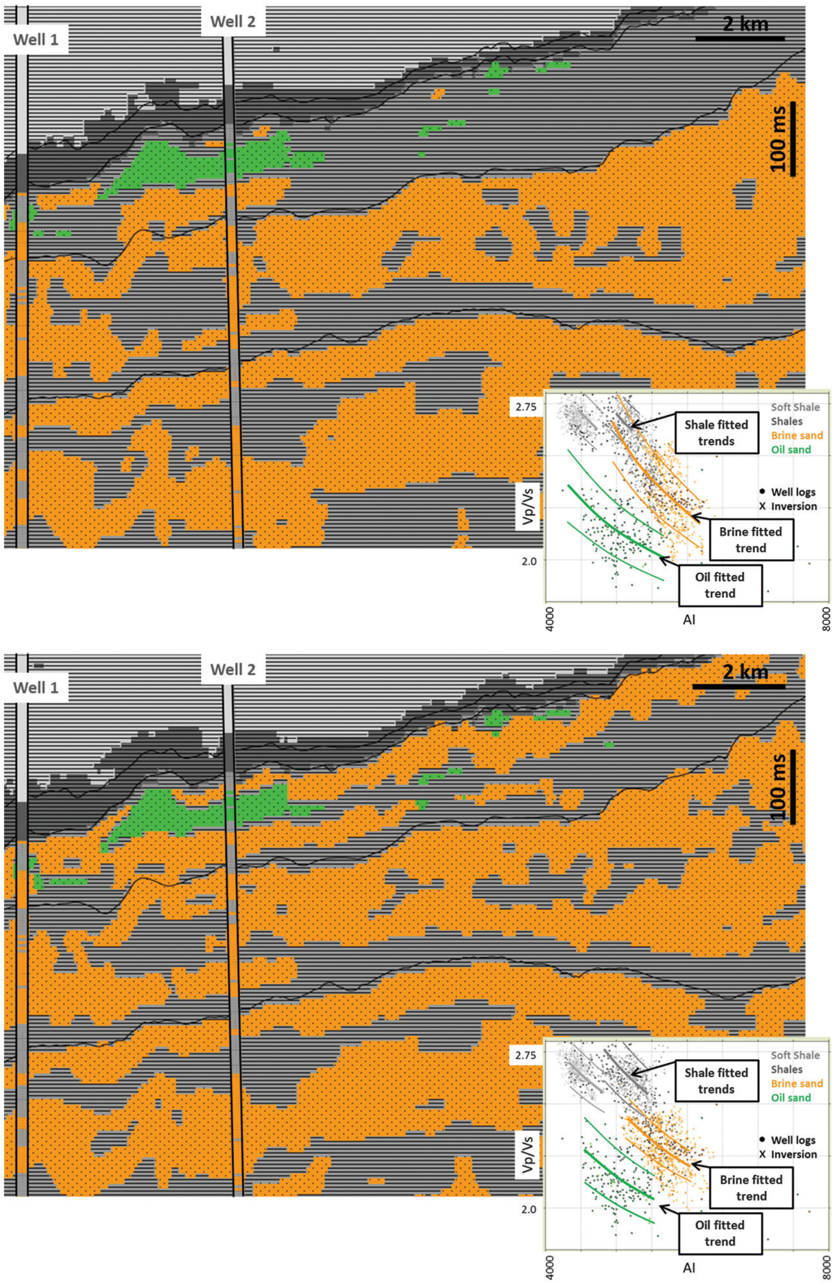

Figure 8. Two scenarios highlight the impact of adjusting the depth-trended RPMs on the inversion result. Even small adjustments have the potential to create significant differences in the inversion result. These sensitivities can be fully explored in multiple inversion runs but ultimately should be calibrated to nearby wells.

produce a range of geologically plausible scenarios. The adjusted parameters typically include the probability proportions of each facies (which we discussed in Figure 6) and also their depth-trended RPMs. In Figure 4, we showed the depth-trended RPMs for the facies used in this study to estimate a low-frequency model for each facies and how these then act as prior information to the inversion. To obtain a credible inversion outcome, these depth-trended RPMs require well control and care in construction. It is good practice to inspect the sensitivity of the RPMs in crossplot space (Figure 7) rather than in the depth trend domain (Figure 4) to visualize and fully understand the separation between facies. From within the elastic crossplot space, we can manually adjust the RPMs to account for variations that may exist outside of the bounds suggested by the calibration wells. Two scenarios are used to demonstrate the importance of this step on the final inversion result. Figure 8 shows the Vp/Vs-AI crossplots for the two selected scenarios. The depth-trended RPMs are displayed on the crossplots and follow the general compaction/porosity trends. Similarly, the error bounds are also projected on the crossplot. The corresponding inversion results generated from these two scenarios are also shown in Figure 8. It can be observed that what might not appear as a big change of the depth-trended RPMs (see the fitted lines of brine and oil sands on the crossplot) has a significant effect on the inverted facies. The separation of the facies from the second scenario allowed a better match of the brine sand at the wells (Figure 8, bottom). In reality, a full range of sensitivities are produced to provide a variety of potential subsurface scenarios, which could then be fully considered and evaluated during future dynamic reservoir modeling studies and development decisions.

Conclusion

Facies-based seismic inversion has been demonstrated, via a North Sea case study, to provide significant advantages over more conventional impedance-only inversion techniques. When facies-based inversion is combined with broadband data and appropriate broadband well tie techniques, the resulting classified facies output provides a result ideally suited for geologic interpretation and the generation of static and dynamic reservoir models. The joint impedance and facies inversion technique successfully

- provides a better facies correlation with calibration wells,
- inverts for an optimum low-frequency model — thereby removing one of the most significant sources of error in more conventional simultaneous inversion techniques, in which a low-frequency model is an input, not an output,
- reduces interpretation burden by producing facies-based output, and
- allows a full range of sensitivities to be explored providing some insight into possible inversion error.

Acknowledgments

The authors would like to thank M. Kemper and K. Waters for their contributions and also D. Alexeenko and F. Brouwer. In addition, we would like to thank Summit E&P (especially R. Saxby for his review) and EnQuest PLC (Summit's partner in the 21/6b Block) technical groups for their useful inputs and permission to publish. Finally, CGG are appreciated for permission to publish results generated from their multiclient CornerStone seismic data set and in particular S. Bowman. Summit Exploration & Production Ltd. is a wholly owned subsidiary of Sumitomo Corporation, Japan.

References

Guillaume, P., X. Zhang, A. Prescott, G. Lambaré, M. Reinier, J. P. Montel, and A. Cavalié, 2013, Multi-layer nonlinear slope tomography: 75th Annual International Conference and Exhibition, EAGE, Extended Abstracts, Th 04 01.

Kemper, M., and J. Gunning, 2014, Joint impedance and facies inversion — Seismic inversion redefined: First Break, **32**, 89–95.

Rutherford, S. R., and R. H. Williams, 1989, Amplitude-versus-offset variations in gas sands: Geophysics, **54**, 680–688, doi: 10.1190/1.1442696.

Wang, P., S. Ray, C. Peng, Y. Li, and G. Poole, 2013, Premigration deghosting for marine streamer data using a bootstrap approach in tau-p domain: 83rd Annual International Meeting, SEG, Expanded Abstracts, 4238–4242.

Zabihi Naeini, E., J. Gunning, and R. E. White, 2016b, Well tie for broadband seismic data: Geophysical Prospecting, **65**, 503–522, doi: 10.1111/1365-2478.12433.

Zabihi Naeini, E., N. Huntbatch, A. Kielius, B. Hannam, and G. Williams, 2015, Mind the gap — Broadband seismic helps to fill the low frequency deficiency: EAGE Workshop on Broadband Marine Seismic, Expanded Abstracts, 25823.

Zabihi Naeini, E., M. Sams, and K. Waters, 2016a, The impact of broadband wavelets on thin bed reservoir characterisation: 78th Annual International Conference and Exhibition, EAGE, Extended Abstracts, WS01 B02.

Biographies and photographs of the authors are not available.